Indian Journal of Chemical Technology
Vol. 30, May 2023, pp. 293-307
DOI: 10.56042/ijct.v30i3.62814

Degradation of Orange G by UV/TiO_2/IO_4^- process: Effect of operational parameters and estimation of electrical energy consumption

Hayet Chamekh[1,2], Mahdi Chiha*[,1], Fatiha Ahmedchekkat[1]& Nour El Houda Souames[1,2]

[1]Laboratory of Anticorrosion-Materials, Environment and Structure (LAMES-E1061500), Chemical Engineering Department, Faculty of Technology, University of 20 Août 1955-Skikda, P.O. Box 26, 21000 Skikda, Algeria.

[2]Laboratoire de Recherche sur la Physico-Chimie des Surfaces et Interfaces (LRPCSI), University of 20 Août 1955-Skikda, P.O. Box 26, 21000 Skikda, Algeria.

E-mail: china_m_f@yahoo.fr

Received 18 September 2022; accepted 28 March 2023

In the present study, the degradation of an azo dye Orange G (OG) by the UV/TiO_2/periodate (IO_4^-) process has been investigated. OG was totally disappears within 10 min by the UV/TiO_2/IO_4^-compared to UV alone, UV/TiO_2 or UV/IO_4^-. A synergistic effect has been obtained when combining the UV/TiO_2 and the UV/IO_4^-systems, resulting in positive interactions between both processes. Experiments conducted with specific hydroxyl radical scavengers, show that despite the inhibition effect observed, complete degradation has been achieved beyond 10 min, demonstrating that the degradation is not only initiated by hydroxyl radical, but also by other reactive entities; the involvement of iodate radical is confirmed with the use of chromium species as a competitor with periodate ions for the photogenerated electron at the conduction band. The operating parameters influencing the degradation process such as initial dye concentration, initial periodate concentration, light intensity/wavelength and initial *p*H solution have been explored. The presence of inorganic ions such as chloride, bromide, sulphate, carbonate and bicarbonate ions in the irradiated solution show reverse effects depending on the concentration used. The OG degradation in different water matrices is found to be sensitive to the presence of different species and their nature. Chemical oxygen demand (COD) has been partially removed after 10 min of treatment, and then this COD abatement stabilized, indicating the strength of the by-products from dye degradation by the UV/TiO_2/IO_4^- system during the treatment time. The electrical energy consumption is estimated at 2.21kWhm^{-3}/Order. The results obtained indicate that the UV/TiO_2/IO_4^- process could be used as a hybrid process to the treatment of dye contaminated water.

Keywords: Energy consumption, Hybrid advanced oxidation process, Hydroxyl radicals, Iodate radicals, Orange G, Periodate

The diminution of fresh water and the deteriorating water quality caused by the wastewater released from different industries have become the most current environmental issues facing by living things over the world[1]. Organic dyes are one of the major sources of water pollution because of their widespread application in industry such as textile, leather, food, cosmetic, pharmaceutical etc[2,3]. These dyes are chemically, photolytically and biologically highly stable, and are highly persistent in nature[4]. Hence, discharge of those colored effluents into natural bodies prevent light penetration, impose biological stress in the water medium and provide an aesthetically displeasing appearance, and can also originate dangerous by-products through oxidation, hydrolysis, or other chemical reactions taking place in the wastewater phase[5,6]. The hazardous, toxic and carcinogenic nature of dyes and their metabolites have been reported in many studies[7,8]. Removal of dye pollutants has therefore become a great challenge, aiming to ensure the sustainability of the environment for future generations by using efficient treatment strategies[9]. The conventional treatment methodologies such as adsorption, flocculation-coagulation, ultrafiltration and reverse osmosis even if they are effective, remain unsuitable for industrial application, since they are non-destructive methods and therefore generate large quantities of sludge which require post-treatment[10]. On the other hand, biological treatment methods do not always provide satisfactory results, due to the large degree of aromatics present in dye molecules and the stability of modern dyes[5]. In this context Advanced Oxidation Processes (AOPs) have received a lot of attention for their efficient degradation of dyes[11]. These methods, primarily based on the formation of highly reactive and oxidative

species, mainly hydroxyl radicals $HO^{\bullet}$, are characterized by being easy to implement, highly efficient, environmentally compatible and able to convert numerous persistent organic pollutants to CO_2, H_2O and inorganic ions[12,13]. Among various AOPs, heterogeneous photocatalysis using different photocatalysts has achieved good goals in the removal of dyes from aqueous effluents[14-17]. Photocatalysis is a reaction initiated by the absorption of photons by a semi-conductor as nano-catalyst[18]. Titanium dioxide (TiO_2) is one of the most studied materials in the fields of renewable energy and environmental protection because of its low cost, low toxicity, and chemical inertness[19,20]. When the TiO_2nano-particle absorbs photons with energy higher or equal to its band gap, a conduction-band electron (e^-_{CB}) and a valence-band hole (h^+_{VB}) are then generated (Equation1)[21]. The photoinduced holes oxidize H_2O or OH^- to generate hydroxyl radicals ($HO^{\bullet}$) (Equations 2-3)[22]. The photogenerated electron can be trapped by oxygen to form superoxide ($O_2^{\bullet-}$) and hydroperoxyl radicals ($HO_2^{\bullet}$), and subsequently hydrogen peroxide (H_2O_2) (Equations 4-7)[23].

$$TiO_2 + h\nu \rightarrow e^-_{(CB)} + h^+_{(VB)} \quad ...(1)$$

$$h^+ + H_2O \rightarrow HO^{\bullet} \quad ...(2)$$

$$h^+ + OH^- \rightarrow HO^{\bullet} \quad ...(3)$$

$$e^- + O_2 \rightarrow O_2^{\bullet-} \quad ...(4)$$

$$O_2^{\bullet-} + H^+ \rightarrow HOO^{\bullet} \quad ...(5)$$

$$HOO^{\bullet} + e^- \rightarrow HO_2^- \quad ...(6)$$

$$HO_2^- + H^+ \rightarrow H_2O_2 \quad ...(7)$$

In competition with charge transfers to adsorbed species, the separate electron–hole can easily recombine either in the bulk or at the surface of the catalyst with the release of energy[24]. Thus, the deferring of electron–hole recombination by the addition of electron acceptors such as IO_4^-, $S_2O_8^{2-}$, BrO_3^-, ClO_3^- and H_2O_2 is essential to increase the rate of photocatalysis via (i) increasing the number of trapped electrons; (ii) generation of more hydroxyl radicals and other oxidizing species; (iii) increasing the oxidation rate of the intermediates compounds and (iv) avoiding the problem of low oxygen concentration[25,26].

Although several studies have reported the effects of adding periodate ions (IO_4^-) as inorganic oxidant species to the photocatalysis process[25,27-31], few complete studies have been carried out on the degradation ability of UV/TiO_2/Periodate system. Hence, in this study, the performance of UV/TiO_2/Periodate (UV/TiO_2/IO_4^-) process for the degradation of Orange G in aqueous solution was evaluated. Orange G (OG) is a typical and poisonous azo dye, extensively used in the dyeing of fabrics[32,33]. It has been reported to show chromosomal damage and clastogenic activity as special toxic effect[34,35]. Thus, its widespread utilization can cause a serious problem due to its obvious and latent danger for humans and ecosystem[36]. This prompted us to study its removal using UV/TiO_2/IO_4^- process as mentioned above. In addition to the effect of different operational parameters, the feasibility of the process toward the removal of OG was assessed in term of electric energy consumption. The chemical oxygen demand (COD) for oxidation process was evaluated and compared to the decolorization process. This study, will undoubtedly allow us to position this process as a hybrid on a large scale.

Experimental Section

Materials

Orange G (abbreviation: OG; CAS number: 1936-15-8; CI number: 16230; IUPAC name: disodium; 7-hydroxy-8-phenyldiazenylnaphthalene-1,3-disulfonate; chemical class: azo; molecular formula: $C_{16}H_{10}N_2Na_2O_7S_2$; molecular weight (g/mol): 452.37; solubility (g/L): 80 at 25°C; *p*Ka: 11.5; maximum wavelength: 478 nm) was purchased from RAL diagnostics and used as a target pollutant. The molecular structure of OG is shown in Fig. 1(a).

Periodic acid (H_5IO_6) used as inorganic oxidant species, was purchased from Panreac. Titanium oxide: (TiO_2 Degussa P-25, 55 m^2/g, crystallite size 25–35 nm, 80% anatase and 20% rutile, non-porous, pH_{PZC} = 5.6, (Ref. 37) analytical grade) was used as nanocatalyst. All other reagents (sulfuric acid, sodium hydroxide, sodium bicarbonate, sodium carbonate, sodium chloride, sodium sulfate, potassium bromide, isopropyl alcohol, *tert*-butyl alcohol, methanol, ethanol, chromium trioxide) were chosen from the purest grade available (analytical grade).

All solutions were prepared with distilled water (DW). Some environmental waters namely Tap water (TW), mineral water (MW), spring water (SW), Zemzem mineral water (ZW), Mediterranean Sea water (MW_{sea}) and Dead Sea water (DW_{sea}), were used as aqueous matrices in other experimental series. The main characteristics of these aqueous matrices are presented in Table 1.

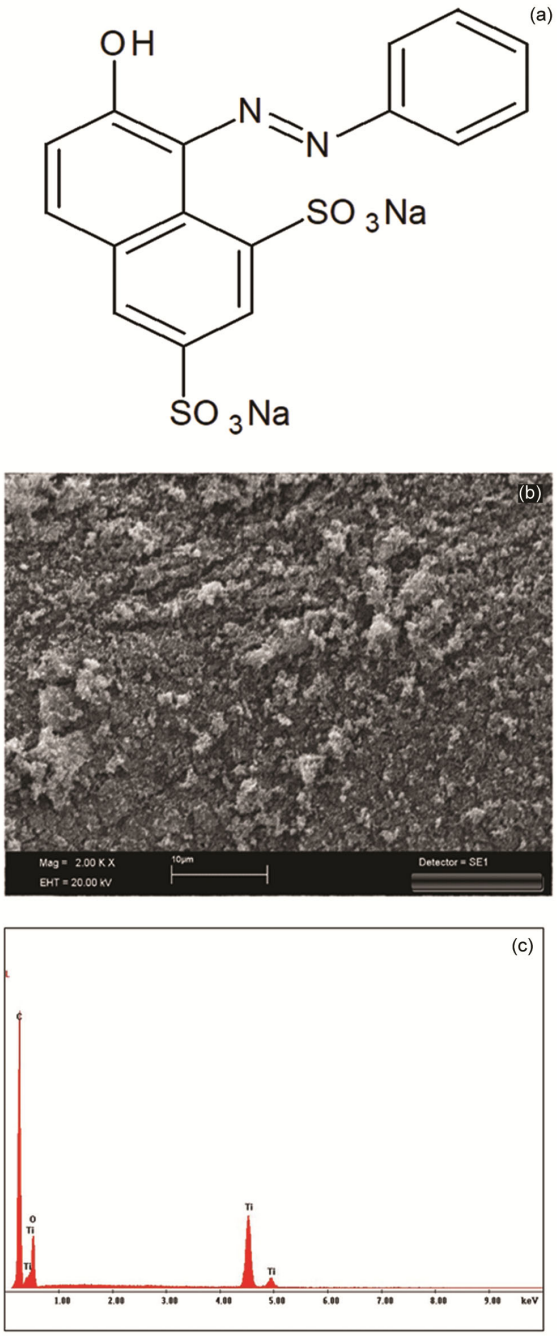

Fig. 1(a) — Chemical structure of Orange G (OG); (b) The morphology image ofTiO_2 nanoparticles carried out at a magnification of 50000 times and (c) EDX spectrum of the commercial nanoparticles from the entire area is shown in SEM image carried out at a magnification of 50000 times.

Photo-reactor

Experiments were conducted in a cylindrical water-jacketed reactor with a volume capacity of 500 mL. A 6.5 W low-pressure mercury UV lamp (Lamp 1: intensity = 4750 µW/cm²) with a maximum emission wavelength of 254 nm and a lower emission wavelength of 184.9 nm was completely immersed in axial position inside the cylindrical reactor. Two others UV lamps were used in others experiments (Lamp 2: λ = 254 nm, intensity = 5400 µW/cm²; Lamp 3: λ = 365 nm, intensity = 1280 µW/cm²). The temperature of the solution was regulated at 20±2°C by circulating cooling water within the jacket surrounding the cell and monitored using a thermocouple immersed in the reacting medium. The reactor content was stirred by a magnetic stirrer. Samples of dye solution were withdrawn periodically from the vessel via a sample port. The set-up used is shown in Fig. 2.

Table 1 — Characteristics properties of aqueous matrices.

Aqueous matrices	Cl^- (mg/L)	Br^- (mg/L)	SO_4^{2-} (mg/L)	HCO_3^- (mg/L)	CO_3^{2-} (mg/L)	*p*H
Tap water	20	/	1.12	372	/	7.4
Mineral water	11	-	7	172	-	7.2
Spring water	97	-	56	357	-	7.6
Zemzem mineral water	147.5	/	610.3	285	/	7.6
Mediterranean sea water*(x10^{-3})*	20	/	265	0.14	/	/
Dead sea water	208	/	0.54	240	/	/

Procedure

The degradation of Orange G by the UV/TiO_2/IO_4^- process was studied in UV-irradiated TiO_2 suspension in the presence of periodate ions. The effect of various operational parameters such as, initial dye concentration, initial periodate concentration, light intensity and/or light wavelength, initial *p*H solution, was investigated by varying one of the parameters, while keeping others constant. A number of assays were carried out to assess the extent of the OG removal in the presence of inorganic ions (Cl^-, Br^-, SO_4^{2-}, HCO_3^- and CO_3^{2-}). The concentration of different inorganic ions was varied over a wide range, in order to estimate the impact of higher concentration on the degradation process. Different types of scavengers (methanol, ethanol, tert-butanol, isopropanol and chromium ions) were used to determine the contribution of the reactive species in the degradation process.

To lead each experiment, OG solution was prepared with the desired initial concentration and *p*H value. Afterwards, a certain amount of the catalyst was added to the solution. Prior to irradiation, the mixture was magnetically stirred for 30 min in the dark in order to reach the adsorption-desorption equilibrium. After this period, the oxidant as well as

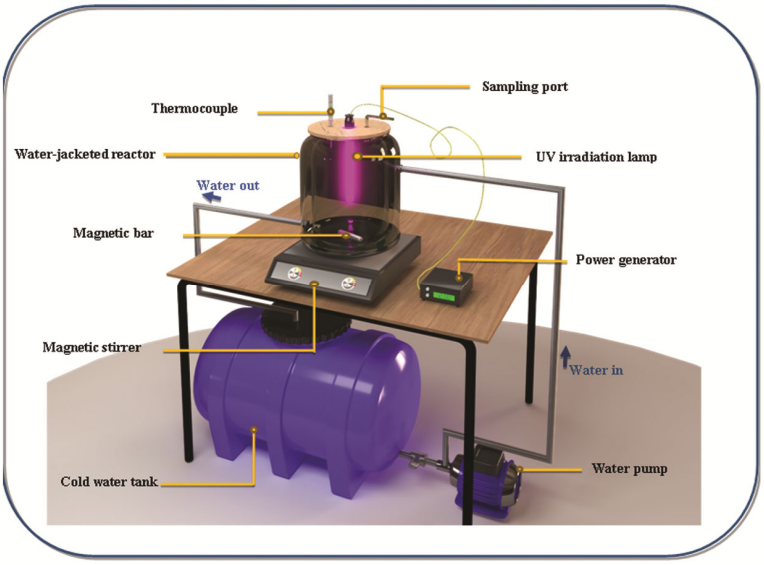

Fig. 2 — Experimental set-up.

other reagents was added to the suspension and the UV lamp was switched on to initiate the process.

Samples were withdrawn periodically and centrifuged at 3000 rpm for 5 min and then filtered to remove the catalyst particles. Residual concentration of OG was determined from its characteristic absorption at 478 nm using a UV-visible spectrophotometer (Agilent Cary 60). The degradation efficiency of OG (R%) was calculated as follow:

$$R\ (\%) = \frac{C_0 - C_t}{C_0} \times 100 = \frac{A_0 - A_t}{A_0} \times 100 \quad ...(8)$$

Where C_0 and C_t are dye concentrations at the initial time and the defined time t respectively; A_0 and A_t are dye absorbance at the initial time and the defined time t respectively.

Chemical oxygen demand measurement

Chemical Oxygen Demand (COD) was measured according to the method presented by Thomas and Mazas[38] using a dichromate solution as the oxidizing agent in a strong acid medium. Test samples (2 mL) were transferred into the dichromate reagent and digested at 148°C for 120 min. The concentration was determined by measuring the optical density using UV–vis spectrophotometer (Agilent Cary 60) at 440 nm.

Characterization of TiO_2nano-particles

Figures 1(b-c) show the morphology and surface features of TiO_2 by scanning electron microscopy (SEM)equipped with an Energy Dispersive X-ray (EDX). In the mentioned figure, spherical structure of the nanoparticles of catalyst with a size between 22 to 100 nm can be seen. Is typical SEM image of TiO_2 nanoparticles. The morphology of the surfaces of the catalyst nanoparticles, namely the commercial TiO_2 - Degussa P-25 used in this study is shown in the images taken using a SEM of the type (Jeol-2100). From these figures, the morphological imaging of the TiO_2 powder, carried out with a magnification of 50000 times [Fig.1(b)] and showed the presence of several agglomerates of nanocatalysts. The phenomenon of formation of these several agglomerates is probably due to the existence of important forces of adhesion, and which interacts between the singular nanoparticles by unit of mass of the powder. Appearance of large adhesion effects between the produced nanoparticles of titanium oxide, flows the significant surface area of the powder (the ratio of the total surface area of the nanoparticles forming the powder into its mass) the dispersion spectra of the X-EDX radiation were obtained. These spectra revealed the presence of oxide and titanium [Fig. 1(c)]. The peak showing the presence of carbon in the sample most likely comes from the carbon ribbon on which the catalyst nanoparticles are fixed.

Results and Discussion

Degradation of OG under UV, UV/IO_4^-, UVTiO_2 and UV/TiO_2/IO_4^-processes

The degree of OG degradation as a target organic pollutant with an initial concentration of 50 mg/L, was carried out under different experimental

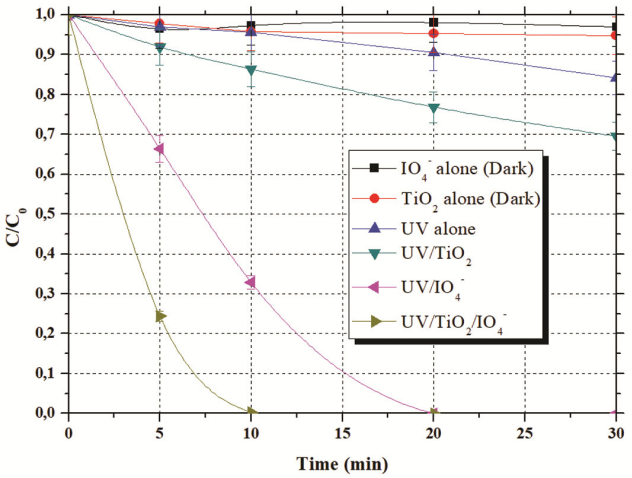

Fig. 3 — Degradation of OG under different advanced oxidation processes (Operating parameters- UV Irradiation: Lamp 1: $\lambda_{254\ nm}$, intensity: 4750 µW/cm²; initial dye concentration: 50 mg/L; periodate concentration: 10^3 mg/L; TiO_2 amount: 4×10^2mg/L; Volume: 400 mL; *p*H: natural (~ 6.5); Temperature: 20± 2°C).

conditions that include: (i) UV alone, (ii) UV/IO_4^- process in the presence of 10^3 mg/L maximum periodate concentration, (iii) UV/TiO_2 process with 4×10^2 mg/L optimum loading of TiO_2, and (iv) UV/TiO_2/IO_4^- in the presence of maximum concentration of periodate (10^3 mg/L) and optimum loading of TiO_2 (4×10^2 mg/L).

The results presented in Fig. 3 showed that approximately 16% degradation of the initial substrate concentration was achieved after 30 min of treatment time when photolysis was applied (UV alone). However, the photo-irradiation in the presence of periodate resulted in complete degradation, i.e. 100% of OG was removed within 20 min of treatment. The observed result in the UV/IO_4^- system can be adequately attributed to the formation of highly reactive radical and non-radical intermediates species under photolysis of periodate in aqueous solution (Equations 9-18)[39,40].

$$IO_4^- + h\nu \rightarrow IO_3^{\bullet} + O^{\bullet-} \quad ...(9)$$

$$O^{\bullet-} + H^+ \leftrightarrow HO^{\bullet} \quad ...(10)$$

$$IO_4^- + HO^{\bullet} \rightarrow IO_4^{\bullet} + OH^- \quad k=4.5\times10^8 M^{-1}s^{-1} \quad ...(11)$$

$$2IO_4^{\bullet} \rightarrow I_2O_8 \quad ...(12)$$

$$2IO_3^{\bullet} \leftrightarrow I_2O_6 \quad k=4.0\times10^8 M^{-1}s^{-1} \quad ...(13)$$

$$I_2O_6 + H_2O \rightarrow IO_4^- + IO_3^- + 2H^+ \quad k=4.5\times10^8 M^{-1}s^{-1} \quad ...(14)$$

$$I_2O_8 + H_2O \rightarrow IO_4^- + IO_3^- + 2H^+ + O_2 \quad k=1.5\times10^8 M^{-1}s^{-} \quad ...(15)$$

$$IO_4^- + h\nu \rightarrow IO_3^- + O \quad ...(16)$$

$$O_2 + O \rightarrow O_3 \quad k=4.0\times10^9 M^{-1}s^{-1} \quad ...(17)$$

$$O_3 + IO_3^{\bullet} \rightarrow IO_4^{\bullet} + O_2 \quad ...(18)$$

Table 2 — Apparent reaction constants obtained in the OG degradation by using different AOPs and the synergy index of the combined process.

Process	[IO_4^-] (mg/L)	K_{app} (min^{-1})	SI
UV/TiO_2	0	0.011	-
UV/IO_4^-	50	0.029	-
	100	0.040	-
	200	0.062	-
	500	0.085	-
	1000	0.105	-
	2000	0.114	-
UV/TiO_2/IO_4^-	50	0.122	0.67
	100	0.243	0.79
	200	0.250	0.71
	500	0.259	0.63
	1000	0.282	0.59
	2000	0.239	0.47

As represented in Fig. 3, there was a negligible loss of the dye when control experiment was carried out with maximum concentration of IO_4^- in the absence of UV irradiation.

In the UV/TiO_2 system, the results obtained (30% of OG removal) showed that TiO_2 photocatalysis was more appropriate than UV alone, which was probably due to the involvement of e^-, h^+ and $HO^{\bullet}$ in the OG degradation process. It should be noted that the dye removal on the nano-catalyst in dark was less than 5%.

The addition of periodate to the UV/TiO_2 system has given the highest rate degradation in a shortest time, where complete degradation was obtained within 10 min. The degradation of OG follows pseudo-first order kinetics for all the processes (data plot no shown), and the corresponding apparent reaction rate constants (k_{app}) are presented in Table 2. The synergistic index calculated for the UV/TiO_2/IO_4^- process using Equation 19[41] (ratio of the difference between the rate constant of the combined process and the sum of those obtained under separate processes, and the rate constant of the combined process) was found to be positive (Table 2), which suggests that the combination of the individual processes provides a synergistic effect, in other words, the presence of positive interactions between both UV/TiO_2 and UV/IO_4^- systems.

$$S = \frac{\left(k_{app(UV/TiO_2/IO_4^-)}\right) - \left(k_{app(UV/TiO_2)} + k_{app(UV/IO_4^-)}\right)}{\left(k_{app(UV/TiO_2/IO_4^-)}\right)} \quad ...(19)$$

Indeed, the incorporation of periodate ions into UV/TiO_2 system prevents the electron-hole recombination by trapping conduction band electron (Equation 20)[42], which in turn leads to the improvement of the photocatalytic process. On the

other hand, this scavenging reaction is followed up by the formation of additional $IO_3^{\bullet}$ radicals, which contribute efficiently in the OG degradation.

$$IO_4^- + 2H^+ + e^- \rightarrow IO_3^{\bullet} + H_2O \quad ...(20)$$

Role of reactive species in the UV/TiO_2/IO_4^-degradation process

Theoretically, ($IO_4^{\bullet}$, $IO_3^{\bullet}$, $O_2^{\bullet -}$,…) and $HO^{\bullet}$ species could be formed when the UV/TiO_2/IO_4^- system is applied in aqueous solution. If hydroxyl radical is a main responsible in the OG degradation, its contribution could be suppressed by using a known $HO^{\bullet}$ radical scavenger in the solution. This method is also valid for indirectly demonstrating the involvement of other reactive entities in the degradation process. Alcohols such as methanol, ethanol, tert-butyl and isopropyl alcohol, are usually used as a diagnostic tool of hydroxyl radicals mediated photocatalytic mechanism[43]. In the present work, the scavenging effect of these alcohols on the elimination of OG was assessed. As shown in Figure 4a, the rate of OG degradation was inhibited in the presence of methanol after 10 min of treatment. Since methanol is an effective scavenger of both h^+ and $HO^{\bullet}$ [44,45], this result suggested that OG could be oxidized by direct interaction with holes or by reaction with $HO^{\bullet}$. The removal of OG was also hindered by the presence of ethanol, tert-butyl and isopropyl alcohols after 10 min (Figs .4b, 4c, and 4d), lending further confirmation for an $HO^{\bullet}$-mediated degradation of the dye. However, despite the inhibition effect, complete OG removal was obtainedbeyond10 min. One might therefore infer that OG does not undergo only hydroxyl radical degradation, but also by the other reactive species generated in the UV/TiO_2/IO_4^- system.

With the use of chromium species (Cr^{VI}) as an electron scavenger, the role of species generated at the reduction band (i.e. $O_2^{\bullet -}$, H_2O_2) (Equations 4-7) could be neglected since Cr^{VI} is easily reduced to Cr^{III} by the photogenerated electron (Equation 21[46]).

$$Cr^{VI} + 3\ e^- \rightarrow Cr^{III} \quad ...(21)$$

As depicted in Fig. 4(e), the presence of chromium species reduced the process efficiency, which suggests the involvement of $O_2^{\bullet -}$species in the OG removal. Another possible explanation is the presence of competition phenomenon between Cr^{VI} and periodate ions to photogenerated electron on the surface of TiO_2 (Equation 21), suggesting that $IO_3^{\bullet}$ could play a crucial role in the OG degradation process.

Effect of operational parameters

Effect of dye concentration

The ability of the UV/TiO_2/IO_4^- system for the degradation of OG was investigated for four different dye concentrations (50 mg/L, 100 mg/L, 150 mg/L and 200 mg/L) in the presence of 4×10^2 mg/L of TiO_2 and 10^3 mg/L of IO_4^-. The obtained results presented in Fig. 5, showed that the percentage removal is inversely proportional to the initial dye concentration. The total elimination of OG was reached after only 10 min for an initial substrate concentration of 50 mg/L, but the removal efficiency decreased to 66, 41 and 27% for 100, 150 and 200 mg/L of dye concentration respectively. This is the consequence of the screen phenomenon which decreases the path length of the light entering the solution[47,48], thus preventing irradiation from reaching both TiO_2 surface and the periodate ions. Also, with the increase in dye concentration, the intermediates molecules formed as a result of degradation process also increase[49]. These intermediates molecules then compete with the dye for the oxidizing entities, which reduces the number of the reactive species available for the dye removal[49]. Thus the [substrate]/[reactive species] ratio becomes insufficient and the efficiency of the process decreases. Furthermore, the degradation rate can be enhanced by increasing the irradiation time, where 95% for 100 mg/L, 96% for 150 mg/L and 96% for 200 mg/L were reached after 100 min and these results are in conformity with previous work[50].

Effect of periodate concentration

The influence of periodate ions concentration on OG degradation in UV/TiO_2/IO_4^-system was evaluated in the range of 50 mg/L to 2×10^3mg/L at natural pH solution (6.5), with 50 mg/L of OG and 4×10^2mg/L of $TiO_2$and compared to the photocatalytic process (i.e. without IO_4^-). Based on the results shown in Fig. 6, the photocatalytic process was enhanced significantly by adding IO_4^- ions to the solution, where total elimination of the substrate was achieved after 70 min of irradiation over the range of periodate concentrations tested. The required time for OG degradation declined from 70 to 10 min with increasing the IO_4^- ions concentration from 50 to 10^3 mg/L respectively, then grew up for excess periodate ions concentration (2×10^3 mg/L).When the periodate

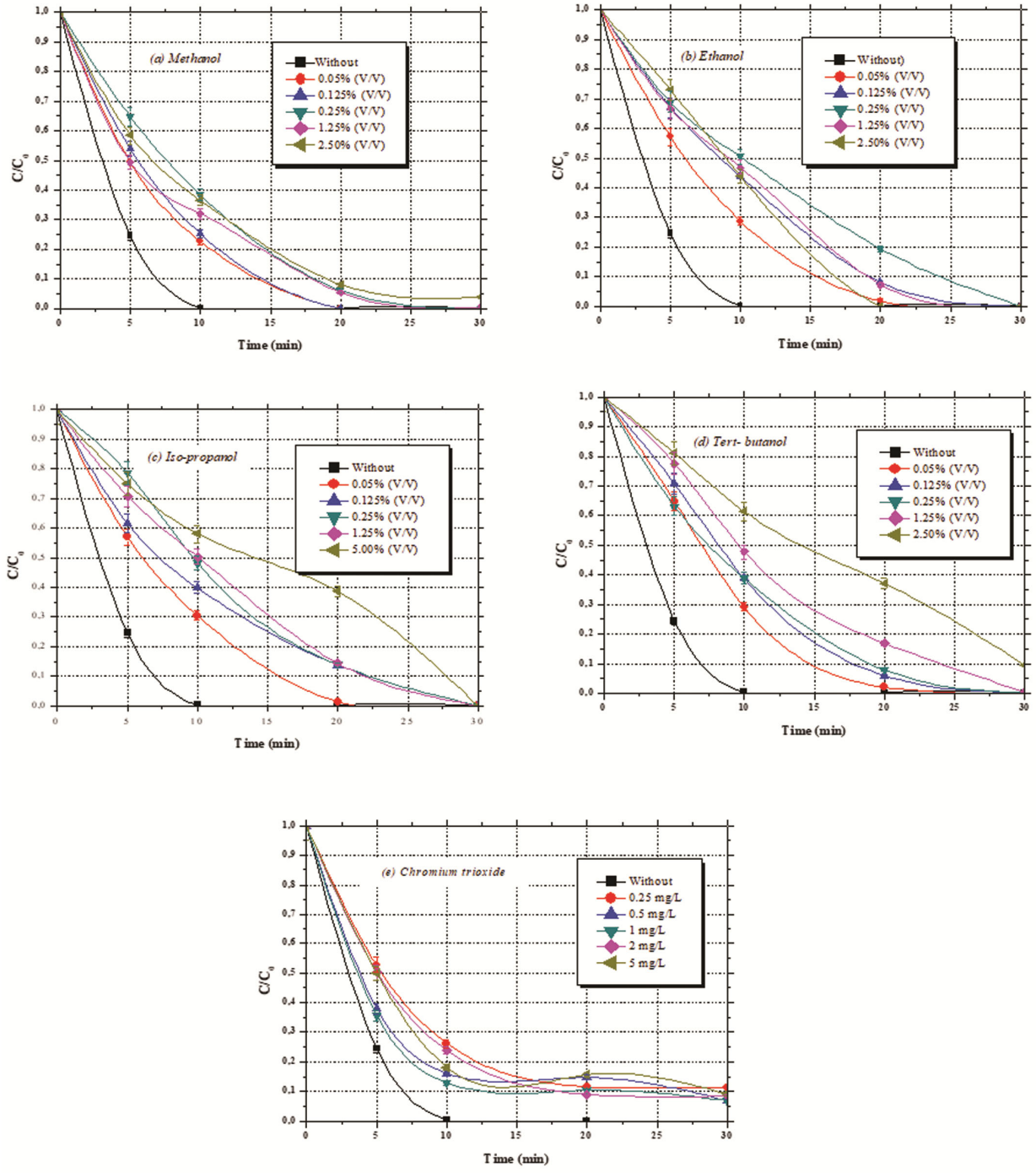

Fig. 4 — Degradation of OG with the UV/TiO_2/IO_4^- process in the presence of (a) methanol; (b)ethanol; (c) tert-butyl; (d) isopropyl; (e) chromium trioxide (Operating parameters- UV Irradiation: $\lambda_{254\ nm}$, intensity: 4750 µW/cm²; initial dye concentration: 50 mg/L; periodate concentration: 10^3 mg/L; TiO_2 amount: 4×10^2 mg/L; Volume: 400 mL; *p*H: natural (~ 6.5); Temperature: 20± 2°C).

concentration increases from 50 mg/L to 10^3 mg/L, more radicals are generated in the solution via the reaction mechanism described in Equations 9,10,16,17,18 and Equation 20, which explain the positive effect of IO_4^- ions on the OG degradation in this range of concentrations. A similar behaviour was observed in the UV/IO_4^- system in our previous work[51]. However, when rising the periodate concentration beyond 10^3 mg/L (i.e. up to $2x10^3$ mg/L), the excess of IO_4^- may quench $HO^\bullet$ and $IO_3^\bullet$ radicals according to Equation 11 and Equation 22[52], which could explain the declined degradation efficiency.

$IO_4^- + IO_3^{\bullet} \rightarrow IO_4^{\bullet} + IO_3^-$ $k=(2\text{-}7)\times10^8 M^{-1}s^{-1}$...(22)

The competition reactions involving $IO_4^{\bullet}$, $IO_3^{\bullet}$with themselves (Equations 12-13) and their reaction with the substrate could also be suggested[53,54]. Also, in the presence of excess periodate concentration; photons could be intercepted by IO_4^-ionsbefore reaching the nanocatalyst surface, which in turn reduce the OG degradation efficiency by the UV/TiO_2/IO_4^- system. An optimum periodate concentration of 1.8×10^3 mg/L was reported by Saien *et al.*[55], for the removal of Furfural by the UV/IO_4^- process.

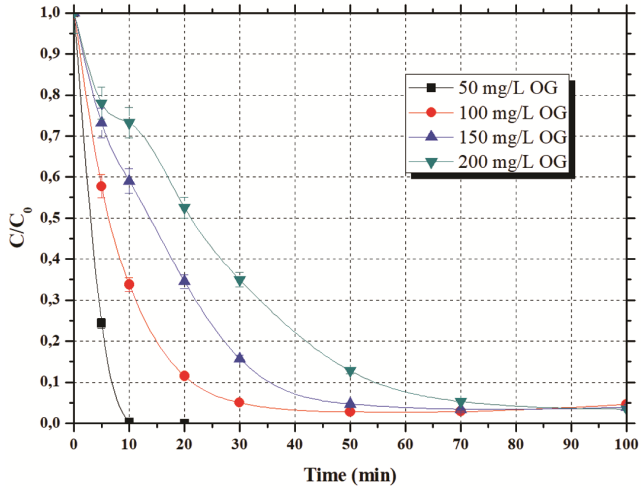

Fig. 5 — Degradation of OG with the UV/TiO_2/IO_4^- process for various dye concentration (Operating parameters-UV Irradiation: Lamp 1: $\lambda_{254\ nm}$, intensity: 4750 µW/cm²; periodate concentration: 10^3mg/L; TiO_2 amount: 4×10^2 mg/L; Volume: 400 mL; *p*H: natural (~ 6.5); Temperature: 20± 2°C).

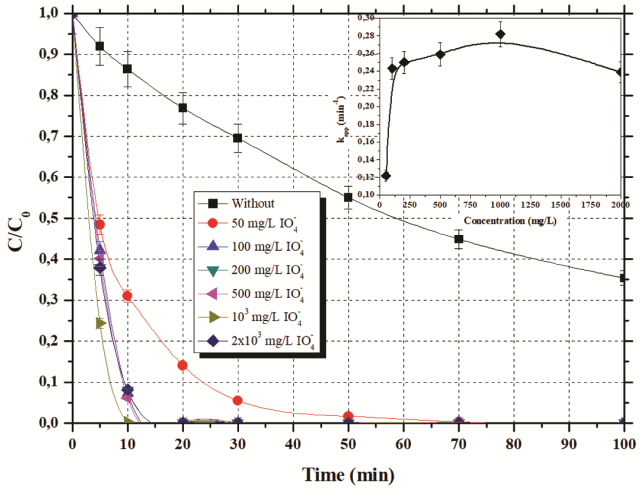

Fig. 6 — Degradation of OG with the UV/TiO_2/IO_4^- process for various periodate concentration (Operating parameters- UV Irradiation: Lamp 1: $\lambda_{254\ nm}$, intensity: 4750 µW/cm²; initial dye concentration: 50 mg/L; TiO_2 amount: 4×10^2 mg/L; Volume: 400 mL; *p*H: natural (~ 6.5); Temperature: 20± 2°C).

Effect of light intensity and light wavelength

The effects of irradiation intensity (I_0) and/or the wavelength (λ) on the OG degradation by UV/TiO_2/IO_4^- system were examined using a UV lamp emitting at 254 nm with a light intensity of 5400 µW/cm² named Lamp 2, and/or a UV lamp emitting at 365 nm with a light intensity of 1280 µW/cm² named Lamp 3, with keeping the others parameters constant (Fig. 7).

Theoretically, the use of high light intensity suggests high absorption energy by the nano-catalyst to produce (e^-–h+) pairs, and at the same time accelerates the homolytic cleavage of the oxidant thus gene[56] rating more reactive species in the reaction medium[57], which could lead to significant effects on the substrate removal. However, the results obtained showed the opposite effect, i.e. the highest is the irradiation intensity (5400 µW/cm²), lowest is the OG percentage removal (97.92 %) obtained with the Lamp 2 compared to 100 % of OG elimination reached with the Lamp 1, having the low irradiation intensity (4750 µW/cm²). This is probably due to the fact that the reactive species generated in a huge amounts in the vicinity of the lamp, are more likely to recombine than to react with the target molecules that are away from the irradiation source. It was reported that a high concentration (e^-–h+) pairs favors their recombination with respect to the required reaction[58].

With the use of the Lamp 3 emitting at 365 nm, 89.39 % of OG removal was achieved after 30 min of irradiation, while 100 % and 97.92 % were reached

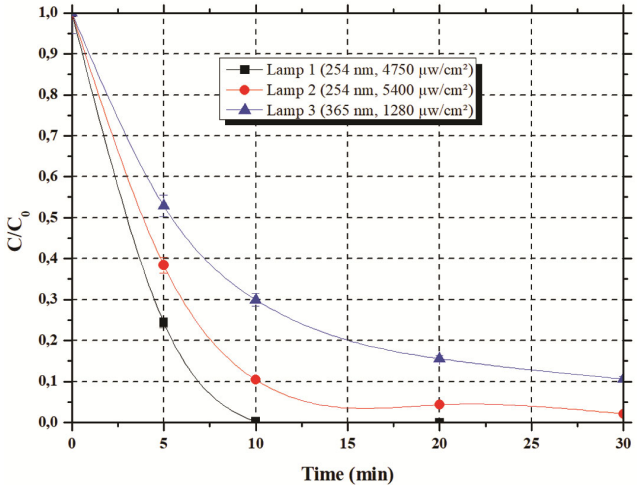

Fig. 7 — Degradation of OG with the UV/TiO_2/IO_4^- process as a function of light intensity and/or wavelength (Operating parameters-initial dye concentration: 50 mg/L; periodate concentration: 10^3mg/L; TiO_2 amount: 4×10^2 mg/L; Volume: 400 mL; *p*H: natural (~ 6.5); Temperature: 20± 2°C).

with Lamp 1 and Lamp 2 respectively, both emitting at 254 nm. This is due to the lower decomposition efficiency of periodate upon 365 nm than upon 254 nm since it absorbs mainly at $\lambda < 300$ nm[59], and therefore fewer reactive species generated. It was reported that the degradation of C.I. reactive red 198in UV/periodate system was 27- and 15-fold much higher under 254 nm than under 365 nm for 1 and 3 mM of IO_4^-, respectively[28].

Effect of initial pH solution

The effect of initial *p*H solution on the OG elimination by UV/TiO_2/IO_4^- system was investigated in the range of 2.6-12, and by fixing the other parameters ([OG] = 50 mg/L, [IO_4^-] = 10^3 mg/L, [TiO_2] = 4×10^2 mg/L) (Fig.8). The obtained results showed that the degradation rate was as 85%, 87%, 86%, 100%, 87% and 55% at *p*H 2.6, 3.1, 4, 6.5(natural *p*H), 8.7 and 12 respectively. In photocatalytic process, the *p*H of the solution affects the ionization state of nanocatalyst surface, hydroxyl radical formation, particles agglomeration and the specification of dye and by-products[60]. Since the point of zero charge (PZC) of the TiO_2 used in this study is 5.4, the TiO_2 surface is positively charged at *p*H<pzc, whereas it is negatively charged at *p*H>pzc. As OG is an anionic dye with sulfonic group, it is negatively charged in aqueous solution[61]. At acidic *p*Hs (2.6, 3.1 and 4), a significant amount of the dye could be expected to adsorb to the nanocatalyst surface due to the electrostatic attraction with TiO_2 nanoparticles[62]. This will result in the blockage of active sites, preventing the photons to reach the catalyst surface. Hence, a small amount of hydroxyl radicals are generated which explain the low rate degradation obtained (85%, 87%, and 86%) at these *p*H values (2.6, 3.1 and 4) compared to 100% of removal obtained at natural *p*H solution. However, when *p*H increase to 6.5 (natural *p*H), hydroxide ions are sufficiently available to be oxidized to $HO^\bullet$ radicals, thus the efficiency of the process is enhanced. Additionally, in this study, with the presence of periodate ions in the UV/TiO_2 system, the solution *p*H could also affect ionization state of IO_4^- ions. Indeed, according to the periodate speciation diagram, IO_4^- ions are the predominant form at *p*H <8[39], which means that the generation of the reactive species via periodate photolysis will be favorable at *p*H values below 8.Consequently, reactive species necessary to the degradation process would be decreasing at higher *p*H[63], resulting in low removal efficiency of OG at *p*H 8.7 and 12.

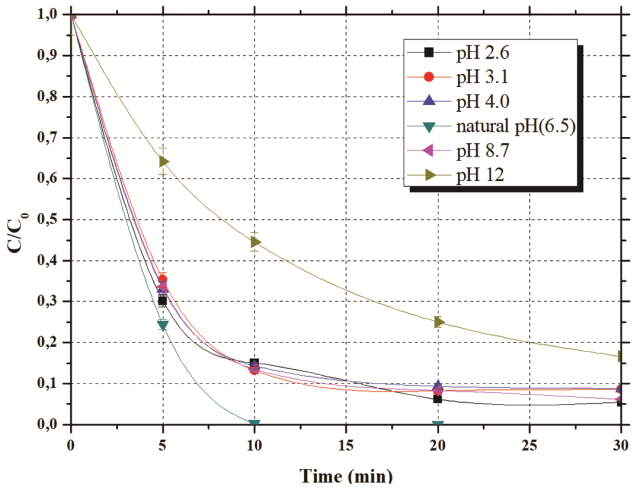

Fig. 8 — Degradation of OG with the UV/TiO_2/IO_4^- process as a function of initial pH solution (Operating parameters- UV irradiation: Lamp 1: $\lambda_{254\ nm}$, intensity: 4750 µW/cm²; initial dye concentration: 50 mg/L; periodate concentration: 10^3 mg/L; TiO_2 amount: 4×10^2 mg/L; Volume: 400 mL; temperature: 20± 2°C).

Effect of inorganic solution anions

The presence of inorganic ions is very common in most aqueous colored solutions as well as in natural water[64]. These inorganic ions are known to react with hydroxyl radicals, or holes, behaving thus as hole or radical scavengers[65], and hence expected to inhibit the efficiency of the treatment by AOPs[64]. However, as a result of such scavenging effect, are produced in the media which could react with the organic substrate, depending on their oxidation potential and selectivity as well as on the reaction kinetics[66]. Hence, it becomes essential to study the neutral, promoting or inhibitory effects which can be caused by the presence of inorganic ions on the contaminant degradation efficiency.

The influence of various inorganic ions namely Cl^-, Br^-, SO_4^{2-}, HCO_3^- and CO_3^{2-}on OG degradation by UV/TiO_2/IO_4^-system was carried out at different concentrations, while keeping the remaining variables constant (50 mg/L of OG, 10^3 mg/L of IO_4^-, 4×10^2 mg/L of TiO_2). The choice of these specific compounds is based on (i)their capacity to produce reactive species by scavenging hydroxyl radicals or holes, and (ii) their presence in wastewater as well as natural water at a considerable quantity, could affect the AOPs process efficiency when applying in real water.

Effect of chloride ions

To evaluate the effect of Cl^- ions on the OG degradation, different concentrations of NaCl ranging

from 30 mg/L to 10×10^3 mg/L were added to the $UV/TiO_2/IO_4^-$ system. As depicted in Fig. 9(a), chloride ions inhibited the degradation efficiency when concentration varied between 30 and 10^3 mg/L. However, the degree of inhibition diminished with increasing the concentration from 30 to 10^3 mg/L. The increase in chloride concentration up to 5×10^3 mg/L exhibited positive effect, but this improvement effect declined as the concentration increased to 10×10^3 mg/L.

Chloride ions in reaction with $HO^\bullet$ and/or h^+ form chlorine radical ($Cl^\bullet$) as shown in Equations 23, 24 and 25[65, 67, 68]:

$$Cl^- + HO^\bullet \leftrightarrow ClOH^{\bullet-} \quad \vec{k}=4.3\times10^9 M^{-1}s^{-1}, \quad \overleftarrow{k}=6.1\times10^9\ s^{-1} \qquad ...(23)$$

$$ClOH^{\bullet-} + H^+ \leftrightarrow Cl^\bullet + H_2O \quad \vec{k}=2.1\times10^{10}\ M^{-1}s^{-1}, \quad \overleftarrow{k}=1\times10^8\ s^{-1} \qquad ...(24)$$

$$Cl^- + h^+ \rightarrow Cl^\bullet \qquad ...(25)$$

This scavenging phenomenon could explain the negative effect observed when NaCl concentration ranged between 30 mg/L and 10^3 mg/L in solution.

However, with increasing NaCl concentration, more chlorine radicals are formed according to the Equations 23-25. As the formed radical $Cl^\bullet$ has a high oxidation potential +2.4V/NHE, it is capable to oxidize organic compounds effectively with a second order rate constant, ranging from $3{,}1\times10^9$ to $4{,}08\times10^{10}$ $M^{-1}s^{-1}$[69].It was reported by Yuan *et al.*[70] that the accumulation of Cl^- could promote the degradation with $Cl^\bullet$ radical-initiated reaction. Thus, the enhancement in OG removal at high concentration (exceeding 10^3 mg/L) may be attributed to the formation of $Cl^\bullet$; this could also explain the decreasing inhibitory degree observed with the increasing concentration from 30 mg/L to 10^3 mg/L.

When the concentration of Cl^- is much important in solution, the generated $Cl^\bullet$ would produce more $Cl_2^{\bullet-}$ (Equation 26). Compared to $Cl^\bullet$,$Cl_2^{\bullet-}$ radical is less reactive towards organic substrates with a second order rate constants ranging from $< 1\times10^6$ to 2.78×10^9 $M^{-1}s^{-1}$ [69]. So excess of Cl^- would reduce the OG degradation rate, as observed when NaCl concentration of $10x10^3$ mg/L was used.

$$Cl^\bullet + Cl^- \leftrightarrow Cl_2^{\bullet-} \quad \vec{k}=8.0\times10^9\ M^{-1}s^{-1}, \ \overleftarrow{k}=6\times10^4\ s^{-1} \qquad ...(26)$$

Chloride ions at high concentration could act as light screen, thereby reducing photon reception efficiency. It is also possible to account for the reduced promoting effect at very high concentration, the hypothesis of the blockage of nanocatalyst active sites by the chloride ions to form an inorganic salt layer[70-72].

Rioja *et al.*[71] reported that under certain conditions, photocatalytic degradation can be achieved in highly saline matrices. According to Ribeiro *et al*.,[73] sodium chloride may produce ambiguous effects on the photocatalytic process depending on the salt concentration and pollutant type.

Effect of bromide ions

The effect of Br^- ions was studied by using different KBr concentrations ranging from 3 to 1000 mg/L. The addition of KBr between 3 and 30 mg/L inhibited the photodegradation process, while above 30 mg/L improvement process was observed [Fig. (9b)]. It is well known that bromide ion reacts with $HO^\bullet$ radical to produce bromine atom ($Br^\bullet$) and dibromide radical anion ($Br_2^{\bullet-}$) (Equations 27-28)[67, 74]:

$$Br^- + HO^\bullet \rightarrow Br^\bullet + OH^- \qquad k=1.1\times10^{10}\ M^{-1}s^{-1} \qquad ...(27)$$

$$Br^- + Br^\bullet \rightarrow Br_2^{\bullet-} \qquad k=9.0\times10^9\ M^{-1}s^{-1} \qquad ...(28)$$

The capture of $HO^\bullet$ radicals by Br^- ions (Equation 27) can explain the inhibition effect observed when concentrations of 3, 5, 10 and 30 mg/L were used. Furthermore, bromide ions at sufficiently high concentration (i.e. above 30 mg/L), could be able to reach the interfacial region of the nanocatalyst through mass transfer phenomenon, and therefore react with $HO^\bullet$ radicals to produce more $Br^\bullet$ and $Br_2^{\bullet-}$ via Equations 27 and 28. Although the $HO^\bullet$ radicals are consumed in the presence of bromide ions, the amount of $Br^\bullet$ and subsequently $Br_2^{\bullet-}$ radicals increase with increasing bromide ions concentration. This could make $Br_2^{\bullet-}$ radicals more available to react with and degrade the target pollutant with a second order rate constants ranging from $< 10^5$ to $1.18\times10^9 M^{-1}s^{-1}$[75].Consequently, Br^- ions could transform $HO^\bullet$ into less reactive species that could however be involved in the substrate decomposition[76].

Effect of sulphate ions

The influence of SO_4^{2-} ions on the $UV/TiO_2/IO_4^-$ system was conducted by varying Na_2SO_4 concentration from 30 mg/L to 2×10^3 mg/L [Fig.9(c)] and found to inhibit the OG degradation process for all the concentrations interval tested. The hindrance effect is due to the trapping $HO^\bullet$ and h^+ by sulphate ions according to the equations below[77,78]:

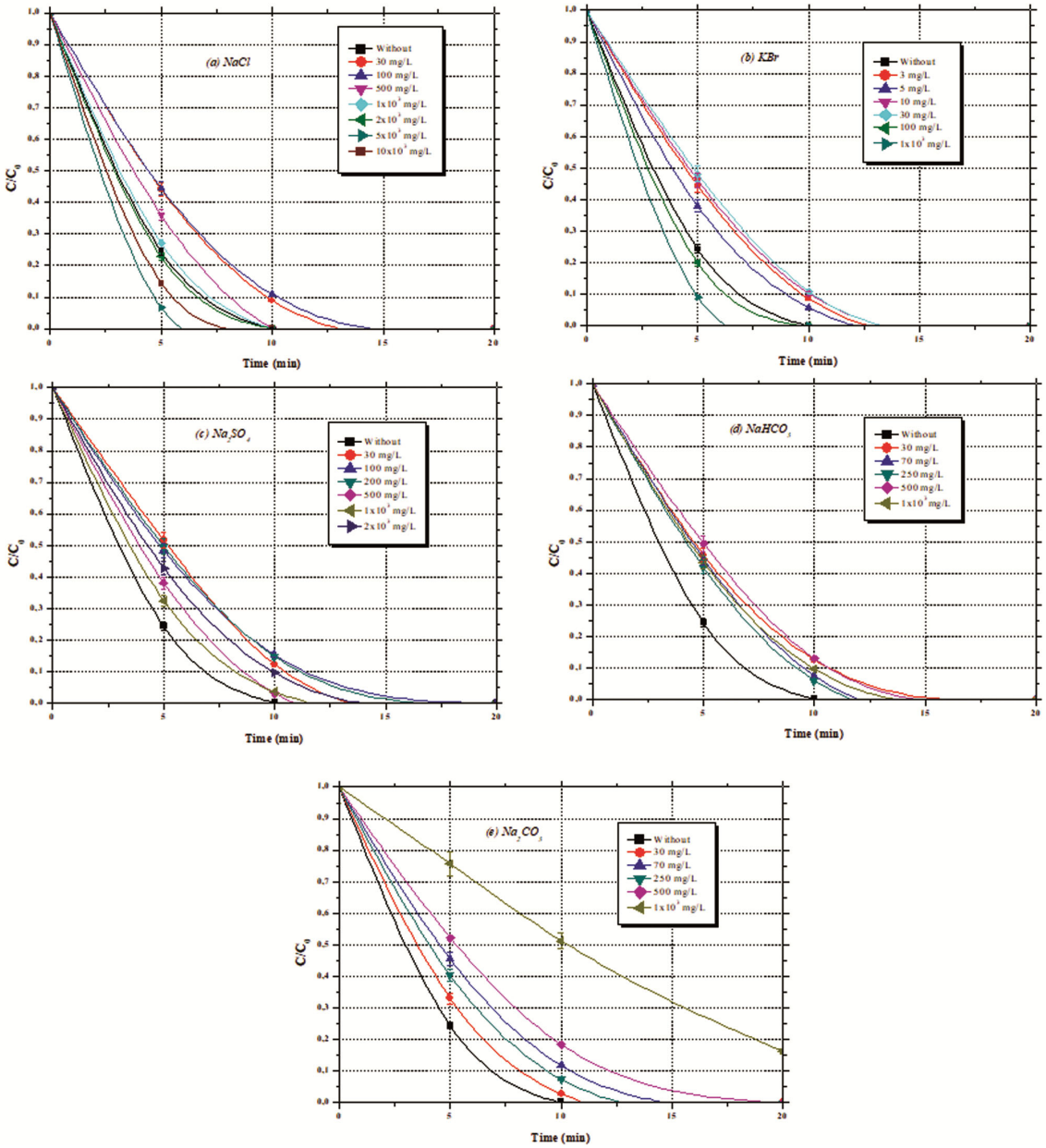

Fig. 9 — Effect of inorganic anions on the OG degradation with the UV/TiO_2/IO_4^- process (Operating parameters- UV irradiation: $\lambda_{254\ nm}$, intensity: 4750 µW/cm², initial dye concentration: 50 mg/L; periodate concentration: 10^3 mg/L; TiO_2 amount: 4×10^2 mg/L; Volume: 400 mL; *p*H: natural; temperature: 20± 2°C).

$$SO_4^{2-} + HO^{\bullet} \rightarrow SO_4^{\bullet-} + OH^- \quad k=1.0\times10^{10}M^{-1}s^{-1} \quad ...(29)$$

$$SO_4^{2-} + h^+ \rightarrow SO_4^{\bullet-} \quad ...(30)$$

Although the formed $SO_4^{\bullet-}$ radical has a high oxidation potential (2.5-3.1 V/NHE), it is selective[79,80], and its large size may render it less effective than $HO^{\bullet}$ radical in the degradation of organic substrates[66].

Effect of bicarbonate and /or carbonate ions

The effect of bicarbonate ions (HCO_3^-) on the OG removal was investigated using $NaHCO_3$ at concentrations ranging from 30 to 1000 mg/L. The obtained result showed a negative impact for all the concentrations range tested [Fig. 9(d)].

The reduction efficiency could be attributed to the reaction of HCO_3^- ions with $HO^{\bullet}$ radicals to produce $CO_3^{\bullet-}$ radicals as described in equation below[67]:

$$HCO_3^- + HO^{\bullet} \rightarrow CO_3^{\bullet-} + H_2O \quad k=8.5\times10^6M^{-1}s^{-1} \quad ...(31)$$

Carbonate ions (CO_3^{2-}) added as Na_2CO_3 at concentrations ranging from 30 to 1000 mg/L inhibited the degradation process mostly at high

concentration [Fig.9(e)]. Like bicarbonate ions, carbonate ions also react with hydroxyl radicals to generate $CO_3^{\bullet-}$ radical (Equation 32)[67],but approximately 45 much times higher, which explains the high inhibition obtained compared to that when bicarbonate ions were used.

$$CO_3^{2-} + HO^{\bullet} \rightarrow CO_3^{\bullet-} + OH^- \quad k=3.8\times10^8 M^{-1}s^{-1} \ldots(32)$$

Carbonate radical is a selective oxidant and reacts more slowly with the organic substrate than $HO^{\bullet}$ radical[81,82], the second order rate constants values are in the 10^2-10^9 $M^{-1}s^{-1}$ range[82].

Although the presence of chloride, bromide, sulphate, carbonate and bicarbonate ions reduced the OG removal rate for mostly the concentrations used, the photo-degradation reaction was still fast enough to complete degradation in acceptable time (i.e. 20 min) and in terms of energy consumption. These results highlight once again the implication of other reactive species in the UV/TiO_2/IO_4^- process. Indeed, if the OG removal was initiated by $HO^{\bullet}$ attack rather than other reactive entities, the impact of different ions would have been more significant since these ions are all $HO^{\bullet}$ scavengers. In addition, these ions could transform $HO^{\bullet}$ into less reactive species that could however be involved into substrate degradation[83] depending on the concentration used.

Degradation of OG in different types of water

The feasibility of OG degradation by the UV/TiO_2/IO_4^- system in natural water, was evaluated using six different types of aqueous matrices namely, tap water (TW), mineral water (MW), spring water (SW), Zemzem mineral water (ZW), Mediterranean Sea water (MWsea) and Dead Sea water (DWsea). As depicted in Fig. 10, an inhibition effect was obtained with all environmental waters used. It should be noted that the strong inhibition effect was obtained with the Dead Sea water. Since natural water behaves a complex mixture of constituents, it is difficult to find out which one played more negative impact in the degradation process[84]. The presence of different inorganic ions such as Cl^-, Br^-, SO_4^{2-}, $HCO_3^-$and CO_3^{2-} at different concentration combined with other compounds ubiquitous in natural water might explain the inhibitory effect observed.

Mineralization assessment

Chemical oxygen demand (COD) is commonly used to indirectly measure the amount of organic compounds chemically oxidisable in liquid waste. [85] In other words, it allows the mineralization degree of

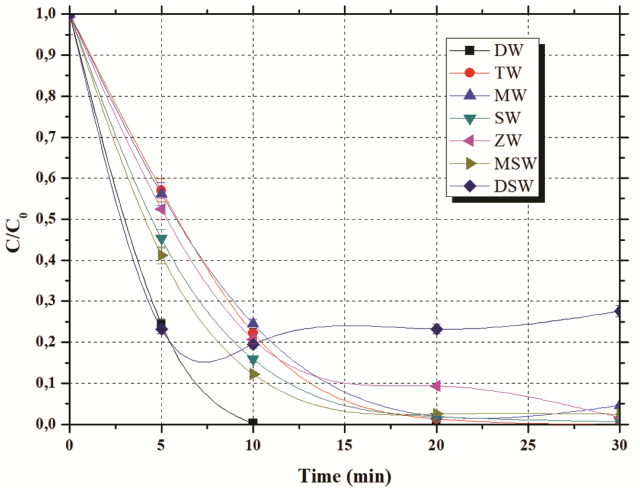

Fig. 10 — Degradation of OG with the UV/TiO_2/IO_4^-process in different water matrices (Operating parameters- UV irradiation: $\lambda_{254\ nm}$, intensity: 4750 µW/cm²; initial dye concentration: 50 mg/L; periodate concentration: 10^3 mg/L; TiO_2 amount: 4×10^2 mg/L; Volume: 400 mL; *p*H: natural; temperature: 20± 2°C).

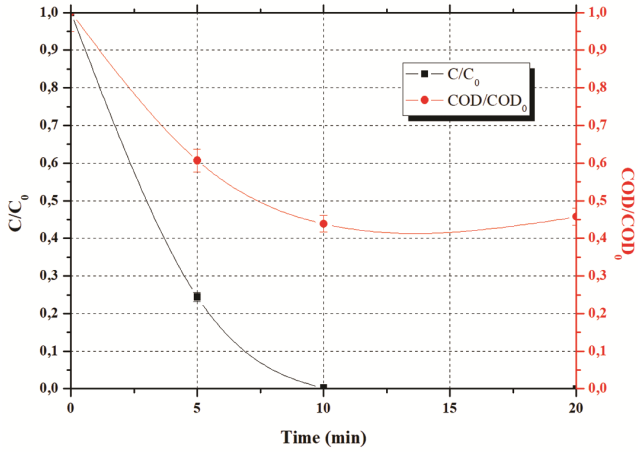

Fig. 11— COD abatement during the OG Degradation with the UV/TiO_2/IO_4^-process (Operating parameters- UV irradiation: $\lambda_{254\ nm}$, intensity: 4750 µW/cm²; initial dye concentration: 50 mg/L; periodate concentration: 10^3 mg/L; TiO_2 amount: 4×10^2 mg/L; Volume: 400 mL; *p*H: natural (~ 6.5); Temperature: 20± 2°C).

the compound to be evaluated. Thus, under the same optimal OG degradation conditions by the UV/TiO_2/IO_4^- system, the evolution of COD abatement was investigated. As can be seen from Fig. 11, the OG degradation resulted in a decrease in COD value indicating the mineralization evolution, and then stabilized. The OG mineralization is a slow process compared to that of degradation. In fact, COD decrease was about 56.15%, while rate degradation was 100% after 10 min. This result means that initial OG molecule breaks down into organic intermediates

that are recalcitrant to the UV/TiO_2/IO_4^- process. At this level, the low mineralization yield might be acceptable, depending on the purpose of the treatment.

Electrical energy consumption

Among the number of important factors in selecting a waste water technology, economics is often paramount and mainly is concerned the electrical energy consumption, most particularly in the case of an electric-energy-driven process like photodegradation[54,86]. Hence, simple figures-of-merit based on electric energy consumption can be very useful and informative[86]. Conventionally, the electric energy required to degrade a contaminant by one order of magnitude in a unit volume of contaminated water defined as E_{EO} (kWhm^{-3}/Order) can be calculated by the equation recommended by the photochemistry commission of the International Union of Pure Applied Chemistry (IUPAC)[87]:

$$E_{EO} = \frac{1000 \times P.t}{60 x V x \log\frac{C_0}{C_f}} \quad \ldots(33)$$

Where P is the electric power (kW); V is the volume of the solution (L); C_0 and C_f are respectively the initial and final concentration (M) of the pollutant, and log is the symbol for the decadic logarithm. For a pseudo-first order reaction, this equation can be simplified:

$$E_{EO} = \frac{38.4 \times P}{V \times k_{app}} \quad \ldots(34)$$

Where k_{app} is the pseudo-first-order reaction rate constant (min^{-1}).

Accordingly, under the same operational conditions of the UV/TiO_2/IO_4^- process (i.e. [OG] = 50 mg/L, [IO_4^-] = 10^3 mg/L; [TiO_2] = 4×10^2 mg/L, 6.5 W light source, 400 mL of treated solution) and considering the pseudo-first-order reaction of 0.282 min^{-1}, E_{EO} was calculated as 2.21 KWhm^{-3}/order. In the case of COD abatement, E_{EO} was calculated as 6.30 kWhm^{-3}/order considering the pseudo-first-order reaction of 0.099 min^{-1}. Generally, speaking an E_{EO} value equal or less than 10 kWm^{-3}/order is considered as an economically acceptable power requirement for commercial application[23, 88].

Conclusion

The present work demonstrates the potential of the combined AOP process UV/TiO_2/IO_4^- for the elimination of an azo dye Orange G in aqueous solution. The obtained results reveal that the removal efficiency is enhanced using UV/TiO_2/IO_4^- process as compared to UV alone, UV/TiO_2 and UV/IO_4^- processes. Combining UV/TiO_2 and UV/IO_4^- processes gave a synergistic effect. With the use of specific hydroxyl scavengers, the involvement of other reactive species has been confirmed. The degradation efficiency is found to decrease with increasing dye concentration. The removal efficiency increased with increasing periodate ions concentration up an optimum. UV/TiO_2/IO_4^- process is efficient at low light intensity and at 254 nm. Natural *p*H has given the best degradation rate with total elimination. The addition of NaCl, KBr, Na_2SO_4, $NaHCO_3$ and Na_2CO_3 in the degradation process show ambiguous effects, depending on the nature and the concentration of the salt used. The OG degradation is found to be sensitive to the aqueous matrix nature, confirmed the role of the co-existents constituents of water like inorganic ions in the degradation process. In the UV/TiO_2/IO_4^-system, the COD reduction is 56.15% after 10 min of treatment, and the energy consumption E_{EO} is calculated as 2.21 kWhm^{-3}/order. Accordingly, the UV/TiO_2/IO_4^- system could be considered as a promising technique for the treatment of azo dye contaminated water, in terms of both technical performance and cost-effectiveness.

Acknowledgements

The authors would like to thank the Ministry of Higher Education and Scientific Research of Algeria forgenerous finance support of this research project under Contract No.A16N01UN210120190003.

Declaration of interest statement

The authors declare that they have no known competing financial interests or personal relationships that could have appeared to influence the work reported in this paper.

References

1 Kohantorabi M, Giannakis S, Gholami M R, Feng L & Pulgarin C A, *Appl Catal B: Environ*, 244 (2019) 983.
2 Al-Shehri H S, Almudaifer E, Alorabi A Q, Alanazi H S, Alkorbi A S & Alharthi F A, *Environ Pollut Bioavailab*, 33 (2021) 214.
3 Pagano M, Ciannarella R, Locaputo V, Mascolo G & Volpe A, *J Environ Sci Health Toxic/Hazard Subst Environ Eng*, 53 (2018) 393.
4 Nidheesh P V, Zhou M & Oturan M A, *Chemosphere*, 197 (2018) 210.
5 Matoh L, Žener B, Korošec R C & Štangar U L, *27-Photocatalytic water treatment*, Nanotechnology in Eco-

efficient Construction, 2nd Edn, Pacheco-Torgal F, Diamanti M V, Nazari A, Granqvist C G, Pruna A & Amirkhanian S, Eds. Woodhead Publishing, (2019) 675.
6 Arivoli S, Deva M T & Prasath M, *Orbital: Electron J Chem*, 1 (2009)138.
7 Ventura-Camargo B & Marin-Morales M, *TLIST*, 2 (2013) 85.
8 Dutta S, Gupta B, Srivastava S K & Gupta A K, *Mater Adv*, 2 (2021) 4497.
9 Lellis B, Fávaro-Polonio C Z, Pamphile J A & Polonio J C, *Biotechnol Res Innov*, 3 (2019) 275.
10 Muniyasamy A, Sivaporul G, Gopinath A, Lakshmanan R, Altaee A, Achary A & Velayudhaperumal Chellam P, *J Environ Manage*, 265 (2020)110397.
11 Nippatlapalli N & Philip L, *Advanced Oxidation Processes for Dye Removal*, Advanced Removal Techniques for Dye-containing wastewater; Muthu S S & Khadir A, Eds. Springer Singapore: Singapore, (2021) 71.
12 Tarkwa J B, Acayanka E, Jiang B, Oturan N, Kamgang G Y, Laminsi S & Oturan M A, *Appl Catal B: Environ*, 246 (2019) 211.
13 Xia X, Zhu F, Li J, Yang H, Wei L, Li Q, Jiang J, Zhang G & Zhao Q, *Front Chem*, 8 (2020) 1.
14 Liu T, Wang Z, Wang X, Yang G & Liu Y, *Int J Biol Macromol*, 182 (2021) 492.
15 Rafiq A, Ikram M, Ali S, Niaz Fm Khan Mm Khan Q & Maqbool M, *J Ind Eng Chem*, 97 (2021) 111.
16 Lau G E, Che Abdullah C A, Wan Ahmad W A N, Assaw S & Zheng A L T, *Catalysts*, 10 (2020) 1129.
17 Elami D & Seyyedi K, *J Environ Sci Health Toxic/Hazard Subst Environ Eng*, 55 (2020) 193.
18 Byrne C, Subramanian G & Pillai S C, *J Environ Chem Eng*, 6 (2018) 3531.
19 Badvi K & Javanbakht V, *J Clean Prod*, 280 (2021) 124518.
20 Yang K, Dai Y & Huang B, *Catalysts*, 10 (2020) 972.
21 Guo Q, Zhou C, Ma Z & Yang X, *Adv Mater*, 31 (2019) 1901997.
22 Zhu D & Zhou Q, *Environ Nanotechnol Monit Manag*, 12 (2019) 100255.
23 Linden K G & Mohseni M, 2.8 - Advanced Oxidation Processes: Applications in Drinking Water Treatment, *Comprehensive Water Quality and Purification*; edited by S Ahuja, Elsevier: Waltham, (2014) 148.
24 Qian R, Zong H, Schneider J, Zhou G, Zhao T, Li Y, Yang J, Bahnemann D W & Pan J H, *Catal Today*, 335 (2019) 78.
25 Sadik W A, El-Demerdash A G M, Nashed A W, Mostafa A A & Hamad H A, *J Mater Res Technol*, 8 (2019) 5405.
26 Hazime R, Nguyen Q H, Ferronato C, Salvador A, Jaber F & Chovelon J M, *Appl Catal B: Environ*, 144 (2014) 286
27 Ravichandran L, Selvam K & Swaminathan M, *Sep Purif Technol*, 56 (2007) 192.
28 Wu M C & Wu C H, *React Kinet Mech Catal*, 104 (2011) 281.
29 Gozmen B, Kayan B, Gizir A M & Hesenov A, *J Hazard Mater*, 168 (2009) 129.
30 Yu C H, Wu C H, Ho T H & Andy Hong P K, *Chem Eng J*, 158 (2010) 578.
31 Syoufian A & Nakashima K, *J Colloid Interface Sci*, 317 (2008) 507
32 Thao L T, Nguyen T V, Nguyen V Q, Phan N M, Kim K J, Huy N N & Dung N T, *J Environ Sci*, 124 (2023) 379.
33 Fan Z, Zhang Q, Li M, Sang W, Qiu Y & Xie C, *Environ Pollut Bioavailab*, 31 (2019) 70.
34 Verma P & Samanta S K, *Environ Chem Lett*, 16 (2018) 969.
35 Shehu S, Muhammad A, Babamale H & Zango Z, *J Environ Treat Tech*, 9 (2021) 318.
36 Wang Y, Priambodo R, Zhang H & Huang Y H, *RSC Adv*, 5 (2015) 45276.
37 Ahmedchekkat F, Medjram M S, Chiha M & Al-bsoul M A, *Chem Eng J*, 178 (2011) 244.
38 Thomas O & Mazas N, *Analusis*, 14 (1986)300.
39 Zhang X, Yu X, Yu X, Kamali M, Appels L, Van der Bruggen B, Cabooter D & Dewil R, *Sci Total Environ*, 782 (2021) 146781.
40 Weavers L K, Hua I & Hoffmann M R, *Water Environ Res*, 69 (1997) 1112.
41 Dewil R, Mantzavinos D, Poulios I & Rodrigo M A, *J Environ Manage*, 195 (2017) 93.
42 Choi Y, Yoon H I, Lee C, Vetráková L U, Heger D, Kim K & Kim J, *Environ Sci Technol*, 52 (2018) 5378.
43 Chen B, Yang C & Goh N K, *J Environ Sci China*, 17 (2005) 886.
44 Shen M & Henderson M A, *J Phys Chem Lett*, 2 (2011) 2707.
45 El-Morsi T M, Budakowski W R, Abd-El-Aziz A S & Friesen K J, *Environ Sci Technol*, 34 (2000) 1018.
46 Chen Y, Yang S, Wang K & Lou L, *J PhotochemPhotobiol A: Chem*, 172 (2005) 47.
47 Saggioro E M, Oliveira A S, Pavesi T, Maia C G, Ferreira L F V & Moreira J C, *Molecules*, 16 (2011) 10370.
48 Reza K M, Kurny A S W & Gulshan F, *Appl Water Sci*, 7 (2015) 1569.
49 Mudhoo A, Paliya S, Goswami P, Singh M, Lofrano G, Carotenuto M, Carraturo F, Libralato G, Guida M, Usman M & Kumar S, *Environ Chem Lett*, 18 (2020) 1825.
50 Arshad R, Bokhari T H, Javed T, Bhatti I A, Rasheed S, Iqbal M, Nazir A, Naz S, Khan M I, Khosa M K K, Iqbal M & Zia-ur-Rehman M, *J Mater Res Technol*, 9 (2020) 3168.
51 Chamekh H, Chiha M & Ahmedchekkat F, *Degradation of Orange G by Homogeneous Advanced Oxidation Processes*. In *Recent Advances in Environmental Science from the Euro-Mediterranean and Surrounding Regions*, 2nd Ed.EMCEI 2019. Environmental Science and Engineering; edited by M Ksibi, Springer: Cham, (2021) 207.
52 Chia L H, Tang X & Weavers L K, *Environ Sci Technol*, 38 (2004) 6875.
53 Hamdaoui O & Merouani S, *Sonochem*, 37 (2017) 344.
54 Saien J, Shafiei H & Amisama A, *Environ Prog Sustain Energy*, 36 (2017) 1621.
55 Saien J, Moradi M & Soleymani A R, *Clean Soil Air Water*, 45 (2017) 201600460.
56 Li Y, Sun S, Ma M, Ouyang Y & Yan W, *Chem Eng J*, 142 (2008) 147.
57 Chu W, Wang Y R & Leung H F, *Chem Eng J*, 78 (2011) 154.
58 Lair A, Ferronato C, Chovelon J M & Herrmann J M, *J Photochem Photobiol A: Chem*, 193 (2008) 193.
59 Lee C & Yoon J, *J Photochem Photobiol A: Chem*, 165 (2004) 35.
60 Ertugay N & Acar F N, *Water Treat*, 57 (2015) 9318.
61 Zhou F, Yan C, Liang T, Sun Q & Wang H, *Chem Eng Sci*, 183 (2018) 231.
62 Madhavan J, Grieser F & Ashokkumar M, *Ultrason Sonochem*, 17 (2010) 338.

63 Wang Q, Zeng H, Liang Y, Cao Y, Xiao Y & Ma J, *Chem Eng J*, 407 (2021) 126738.
64 Aleboyeh A, Kasiri M B & Aleboyeh H, *J Environ Manage*, 113 (2012) 426.
65 Eskandarloo H, Badiei A & Behnajady M A, *Ind Eng Chem Res*, 53 (2014) 6881.
66 Burns R A, Crittenden J C, Hand D W, Selzer V, Sutter L L & Salman S R, *J Environ Eng*, 125 (1999) 77.
67 Buxton G V, Greenstock C L, Helman W P & Ross A B, *J Phys Chem Ref Data*, 17 (1988) 513.
68 Gao Y Q, Gao N Y, Yin D Q, Tian F X & Zheng Q F, *Chemosphere*, 201 (2018) 50.
69 Lei Y, Cheng S, Luo N & Yang X, *Environ Sci Technol*, 53 (2019) 11170.
70 Yuan R, Ramjaun S N, Wang Z & Liu J, *Chem Eng J*, 192 (2012) 171.
71 Rioja N, Zorita S & Peñas F J, *Appl Catal B: Environ*, 180 (2016) 330.
72 Ismail L, Ferronato C, Fine L, Jaber F & Chovelon J M, *Environ Sci Pollut Res Int*, 25 (2018) 2651.
73 Lado Ribeiro A R, Moreira N F F, Li Puma G & Silva A M T,*Chem Eng J*, 363 (2019) 155.
74 Neta P, Huie R E & Ross A B, *J Phys Chem Ref Data*, 17 (1988) 1027.
75 Lei Y, Lei X, Yu Y, Li K, Li Z, Cheng S, Ouyang G & Yang X, *Environ Sci Technol*, 55 (2021) 10502.
76 Chiha M, Hamdaoui O, Baup S & Gondrexon N, *Ultrason Sonochem*, 18 (2011) 943.
77 Guillard C, Puzenat E, Lachheb H, Houas A & Herrmann J M, *Int J Photoenergy*, 7 (2005) 1.
78 Santiago D E, Araña J, González-Díaz O, Alemán-Dominguez M E, Acosta-Dacal A C, Fernandez-Rodríguez C, Pérez-Peña J & Doña-Rodríguez J M, *ApplCatal B: Environ*, 156 (2014) 284.
79 Devi P, Das U & Dalai A K, *Sci Total Environ*, 571 (2016) 643.
80 Wojnarovits L & Takács E, *Chemosphere*, 220 (2018) 1014.
81 Lai W W, Hsu M H & Lin A Y, *Water Res*, 112 (2017) 157.
82 Wojnárovits L, Tóth T & Takács E, *Sci Total Environ*, 717 (2020) 137219.
83 Minero C, Pellizzari P, Maurino V, Pelizzetti E & Vione D, *Appl Catal B: Environ*, 77 (2008) 308.
84 Khan J A, He X, Shah N S, Sayed M, Khan H M & Dionysiou D D, *Chem Eng J*, 325 (2017) 485.
85 Kosseva M R, , In *Food Industry Wastes*, 2 nd Edn, Edited by M R Kosseva & C Webb, Academic Press, (2020) 67.
86 Daneshvar N, Aleboyeh A & Khataee A R, *Chemosphere*, 59 (2005) 761.
87 Bolton J R, Bircher K G, Tumas W & Tolman C A, *Pure Appl Chem*, 73 (2001) 627.
88 Parsons S, *Advanced Oxidation Processes for Water and Wastewater Treatment*; IWA, London, (2004).